Investigation of PMSE echoes characteristics using the discontinuous EISCAT UHF observation and its relation with space environment

Abdur RAUF[1], LI Hailong[1*], Safi ULLAH[1], WANG Maoyan[2] & MENG Lin[1]

[1] School of Electronic Science and Engineering, University of Electronic Science and Technology of China, Chengdu 610054, China;
[2] School of Physics, University of Electronic Science and Technology of China, Chengdu 610054, China

Abstract The observations of Polar Mesosphere Summer Echoes (PMSE) were carried out using the sporadic data of EISCAT UHF radar during the summer season from 2004 to 2015. There were 25 h of PMSE echoes with EISCAT UHF radar. PMSE echoes were mostly observed only during the early morning and fore-noon time. Moreover, the PMSE echoes are positively correlated with Lyman α radiation, but the correlation is non-significant. The occurrence of PMSE echoes in the early morning and fore-noon time and there positive correlation with Lyman α radiation suggests that solar radiations might be one important factor for PMSE echoes in this study. Very weak positive, but statistically non-significant correlation is found between PMSE occurrence rate and the local geomagnetic K-indices. It is found that there is a matching between the variation in the occurrence rate of PMSE and noctilucent clouds (NLC) up to some extent and they are positively correlated. This positive correlation might support the earlier proposed idea about the role of ice particle size in producing PMSE echoes at higher frequencies.

1 Introduction

Polar Mesosphere Summer Echoes (PMSE) are strong coherent radar backscatter produced at polar latitude due to the cold summer mesosphere between 80 and 90 km (Ecklund and Balsley 1981; Hoppe et al., 1988). Often PMSE have been observed at VHF (Very High Frequencies) and rarely at UHF (Ultra High Frequencies). For example, in July 2004 and 2005 when PMSE echoes were detected by EISCAT VHF and UHF radars located near Tromsø, Norway (69°35′N, 19°14′E), the occurrence rate of the VHF PMSE is as large as 85.0% whereas the UHF PMSE are much rare with an occurrence rate of 5.3% (Li and Rapp,

2011). One apparently obvious explanation of this phenomenon is that the electron density irregularities induced by neutral air turbulence, which is common in summer and is known to be driven by gravity waves, causes the enhanced radar backscatter echoes (Garcia and Solomon, 1985). But, the typical and even extreme energy dissipation rates of the background neutral air turbulence indicates that the smallest irregularities sizes are much larger than that necessary to match the radar Bragg scattering wavelength (radar half wavelength e.g., ~ 3 m for 50 MHz). Thus, electron density does not have enhanced fluctuations around Bragg scale, because irregularities at this scale are rapidly destroyed by diffusion. However, the fluctuations arising from random thermal motions of electrons, causing incoherent scattering are not destroyed by diffusion.

* Corresponding author, E-mail: hailong703@163.com

It was suggested by Kelley et al. (1987) that the reduction in electron diffusivity through ambipolar forces due to the presence of heavy charged ice particles may be responsible for maintaining the electron density irregularity causing PMSE echoes. When the joint rocket radar observations showed that the active neutral turbulence is occasionally absent inside the PMSE active layers then the doubts about the use of this theory to explain PMSE echoes became widespread (Lübken et al., 1993, 2002). However, recently it has been understood that if there is enough reduction in electron diffusivity due to ambipolar forces of heavy charged ice particles then the electron density irregularities might take long time to relax back to the initial state. This long relaxation time probably allows observing PMSE during the decaying phase of irregularities even the neutral air turbulence is absent (Rapp and Lübken, 2003).

Recently it has been confirmed that the presence of charged dust particles with radii from a few up to a few tens of nanometers play a decisive role for PMSE echoes (Cho and Röttger, 1997; Croskey et al., 2001; Havnes et al., 2001; Mitchell et al., 2001). A number of independent observations supported the relation between radar echoes and ice particles i.e. the observations of low temperature values inside PMSE layers clearly indicates that the observed radar backscatters are produced at heights where the air is supersaturated (Lübken et al., 2002, 2004). A connection between noctilucent clouds (NLC) and PMSE has been suspected (Thomas, 1991; Eremenko et al., 2005; Kaifler et al., 2011) because NLCs are visible due to scattering of solar light by ice particles of larger sizes, charged or not (Gadsden, 1981). The presence of ice particles in polar mesosphere during summer time is one common element for both NLC and PMSE.

These phenomena get considerable attention after the evidence that the occurrence of noctilucent cloud sighting occurred not earlier than the year 1885, during which an enhancement of water content at the mesosphere must have begun because of the huge volcanic eruption in August of 1883, located on Krakatoa; thus associating both NLC and PMSE to global change (Thomas et al., 1989; Thomas and Olivero 2001). For an alternative view and a rebuttal, the readers are referred to Von Zahn (2011) and Thomas et al. (2011), respectively. Since the PMSE (Latteck and Bremer,

2017) and NLC (Fielder et al., 2017) occurrence rate in mesosphere at polar latitudes is increasing, so it has been argued that it may be caused by various factors e.g., methane emission due to anthropogenic activities, increased level of CO_2 (carbon dioxide) emission and changes in the atmospheric circulation pattern (Thomas et al., 1989, 2011; Lübken et al., 2013).

Recently, Li and Rapp have found that PMSE at 224 MHz show a better match with NLC than that at 53.5 MHz (Li and Rapp, 2011). They stated that it may tentatively be interpreted as a meaning that the ice particles sizes at higher frequencies play a more important role for PMSE creation.

The aim of this study is to investigate different characteristics of PMSE echoes during the sporadic observation carried out by EISCAT UHF (930 MHz) radar during summer season along a solar cycle. Different characteristics of PMSE echoes i.e., the temporal variation of PMSE occurrence and its occurrence rate at different altitudes are analyzed. The effect of 3 h geomagnetic K indices on the PMSE occurrence rate is calculated on the basis of 3 h time interval, and solar Lyman α radiation is investigated. Moreover, the PMSE occurrence rate in different years is computed and is compared with NLC occurrence rate.

2   Radar and experiment description

The PMSE observations in this study were carried out using the EISCAT UHF radar located at Ramfjordmoen near Tromsø, Norway (69.6° N, 19.2° E). It is a powerful tool used for investigating the earth ionosphere. It has an operating frequency of 930 MHz with a peak power of 2 MW and a 3 dB beam width of 0.51°. The data acquiring channels of this radar has the altitude range of (60–140 km) with a range resolution of 300 m for experiment mode 'arcdlayer-ht' and altitude range of 19–209 km with a range resolution of 180–360 m for experiment mode 'manda'. The antenna used for transmission and reception is a 32 m steerable parabolic dish. Folkestad et al. (1983) have explained the detailed descriptions of this radar. For the PMSE observations used in this study, the radar ran an operating mode manda and arcdlayer-heating. The details about the experiment modes are given in Table 1.

Table 1   Details of experiment modes

Experiment name	Integration time/s	Code	Baud length/μs	Sampling rate /μs	Subcycle length/ms	Duty cycle
Manda	4.8	Alternating, 61 bit, 128 subcycles	2.4	1.2	1.5	0.098
Arcdlayer-ht	2	Alternating, 64 bit, 128 subcycles	2	2	1.346	0.095

The original data-dumps provided by the EISCAT-experiments are auto-correlation functions. These observations are routinely analyzed off-line in terms of electron number densities (or 'apparent' electron densities particularly for

PMSE region) by using the well documented Grand Unified Incoherent Scatter Design and Analysis Package (GUISDAP) (Lehtinen and Huuskonen, 1996). These 'apparent' electron number densities can be converted to volume reflectivity

using the well-known relation,

$$\eta = \sigma \times N_e \qquad (1)$$

Here, $\sigma = 5\times10^{-29}$ m^2 is half the scattering cross-section σ_e of an electron $(\sigma = \sigma_e \times (1 + T_e / T_i)^{-1} = \sigma_e / 2)$ and N_e is the 'apparent' electron number density (Röttger and LaHoz, 1990). The term 'apparent' electron density means that the signals are not a measure of real electron density but due to coherent scatter of PMSE echoes which adds to the incoherent scattering.

3 Data analysis

So far, in the current literature there are only a few PMSE observations carried out using the EISCAT UHF radar (Thomas et al., 1989; Röttger et al., 1990; Belova et al., 2007; Næsheim et al., 2008; Rapp et al., 2008; Li and Rapp, 2013). By analyzing the sporadic observations carried out by EISCAT UHF radar, PMSE echoes were observed only during July of the years 2004, 2005, 2007, 2008, 2011, 2012 and 2015. PMSE echoes were only observed during June for year 2010, and both in June and July for year 2013. For PMSE observations, we have used the data of two experiment mode, manda and arcdlayer-ht. During the 9 years, the EISCAT UHF radar ran for total of 387.8 h. During night time the radar only ran for 2 d during July 2015 i.e., on 16 July at 21:00:33−23:59:55 UT and on 17 July at 00:59:55−23:06:04 UT. The details about the PMSE detection time is given in Table 2.

Table 2 PMSE time with EISCAT UHF radars during the campaign of 'arcdlayer-ht' in 2004, 2005, 2007, 2008, and 'manda' in 2010–2013, 2015

Year	Month	Day	PMSE time/UT
2004	07	12	09–10
		13	08–10
		14	09–10
2005	07	09	08–10
2007	07	12	09–10
		16	07–08
2008	07	06	14–15
2010	06	07	11–12
2011	07	05	11–12
		11	09–10
		21	07–08
2012	07	02	10–11
2013	06	21	09–10
		22	09–13
		23	10–11
			12–13
	07	26	11–12
2015	07	17	05–08

For investigating the PMSE dependence on geomagnetic activity, it is needed to define the PMSE threshold for this study. The radar echoes having volume reflectivity, $\eta \geq 3.0\times10^{-18}$ m^{-3} at altitude range of 80–90 km were used as PMSE echoes, because Rapp et al. (2008) have already used this threshold. The local geomagnetic K-indices of Tromsø geophysical observatory are used to investigate their effect on PMSE occurrence rate. We have used local K-indices instead of planetary K-indices because we want to investigate the relationship between PMSE and geomagnetic activity at the same location. These K-indices gives information about the variation in horizontal component of earth magnetic field due to energetic particles precipitation. These K-indices are derived from the maximum difference of the horizontal component from the quite day conditions within 3-hour interval.

4 Results

4.1 Temporal variation of PMSE occurrence rate

The PMSE occurrence rate was calculated for each hour having PMSE echoes. For example, the PMSE occurrence rate during the time interval, 09–10 UT was calculated from the ratio of PMSE detection time to the total time for which the radar ran at 09–10 UT during all the 9 years of observations. Figure 1 shows the temporal variation of mean PMSE occurrence rate. From this figure it is clear that PMSE echoes are mostly observed in the early morning and fore-noon hours. In this particular study, no PMSE echoes were observed out of total 25 h of continuous radar observations during night time. The occurrence of PMSE at night time requires some extra source of ionization (e.g., energetic particle precipitation) because the normal D-region is recombined there at night time. Varney et al. (2009) noted that a majority of the nighttime PMSE observed by PFISR in 2007 were accompanied by enhanced E-region ionization from particle precipitation. In this particular study, the occurrence of PMSE in the morning and fore-noon time suggests that the ionization caused by solar radiation might play an important role for the creation of PMSE echoes. An overview of the PMSE observations with respect to season and time of day is shown in Figure 2. Polar mesosphere summer echoes from EISCAT UHF observations were present with diverse occurrence rate only in 25 h from 387.8 h of total observations in 9 years. The detail about PMSE observations time is given in Table 2. The detection of PMSE by UHF radar in very small amount of hours in this study supports the previous investigations about the rare occurrence rate of PMSE based on UHF radar observations. Næsheim et al. (2008) observed a PMSE occurrence rate of ~11% in 2004. Li and Rapp (2011) observed a total PMSE occurrence rate (occurrence of PMSE at least at one altitude) of 5.32% in the years 2004–2005.
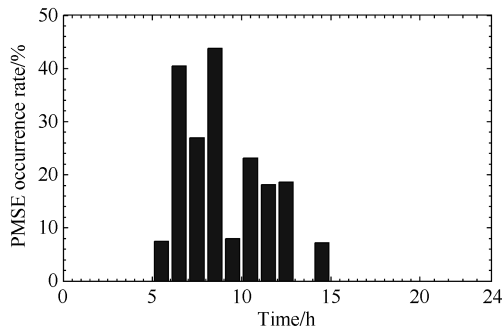
Figure 1   Variation of PMSE occurrence rate with time of the day.
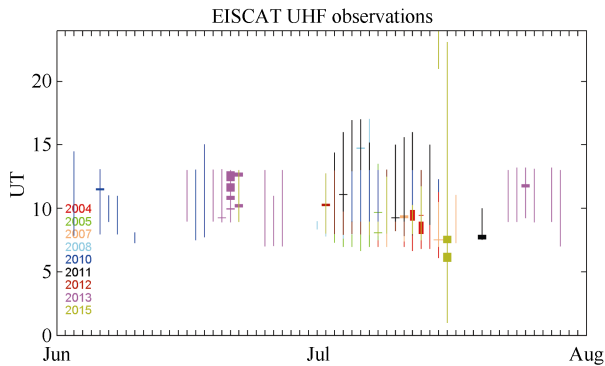

Figure 2   Distribution of observations with respect to season and time of day. The thin and thick lines, respectively represents the unobserved and observed time of PMSE.

4.2   PMSE occurrence rate at different altitudes

Figure 3 shows the altitude profile of PMSE occurrence rate of two different experiment modes. The altitude profile of PMSE occurrence rate is divided into two panels because the UHF radar ran an operating mode 'arcdlayer-ht' for years 2004, 2005, 2007 and 2008 in the upper panel and operating mode 'manda' for years 2011–2013 and 2015 in the lower panel of Figure 3. For both the experiment modes, the PMSE echoes were observed in the altitude range of about 80.4–86.5 km. The detection of PMSE echoes in narrow layers for 9 years of observations is in agreement with the previous findings. For example, Li and Rapp (2011) found that PMSE echoes observed by UHF radar occur in a considerably narrow altitude range of 81–87 km during the simultaneous observations carried out by EISCAT VHF and UHF radar for the years 2004–2005. Li and Rapp (2011) observed that VHF-PMSE occurred with the electron densities at 90 km as low as $5 \times 10^9 \, \mathrm{m}^{-3}$ whereas UHF-PMSE occurred only when the electron densities at 90 km were larger than $1 \times 10^{10} \, \mathrm{m}^{-3}$. Therefore, the requirement of higher electron density for UHF-PMSE occurrence might be one reason for the narrow occurrence of UHF-PMSE. Moreover, in comparison to EISCAT VHF 224 MHz (Bragg scale = 0.67 m), the much shorter Bragg wavelength (0.16 m) of the EISCAT UHF 930 MHz radar seems to be one possible reason for occurrence of UHF PMSE in a considerably narrow altitude range.
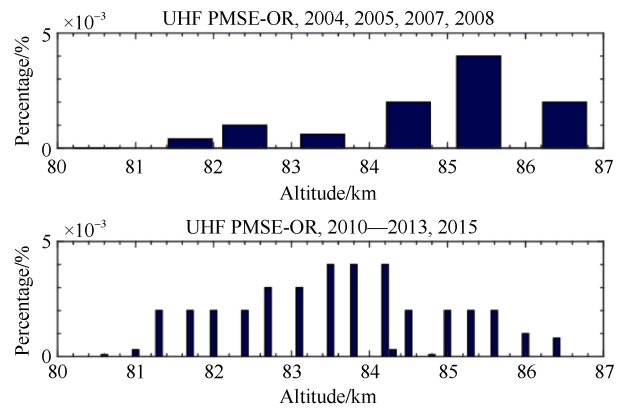

Figure 3   Occurrence rate of PMSE at different heights.

4.3   PMSE occurrence rate and its variation with solar and geomagnetic activity

For the first time we have investigated the effect of geomagnetic activity on PMSE observed by EISCAT UHF radar. The local geomagnetic K-indices of Trømso geophysical observatory have been used to investigate the effect of geomagnetic activity on PMSE occurrence rate.

Since the PMSE observations by UHF radar is scarce, so the PMSE occurrence rate in different years was calculated by considering three-hour time interval corresponding to the 3-hourly geomagnetic K-indices. Since the geomagnetic K-indices gives information about the variation in the horizontal component of earth magnetic field from the quite day conditions within 3-hour interval i.e., during time intervals 00–03, 03–06, 06–09,…, 21–24 UT. Therefore, the PMSE occurrence rate was calculated corresponding to these geomagnetic indices. For example, if the PMSE echoes were observed at any time during the interval, 06–09 UT, then the occurrence rate was calculated from the ratio of PMSE detection time to the total time for which the radar ran during 06–09 UT.

Figure 4 shows the correlation between PMSE occurrence rate and local geomagnetic K-indices. The correlation coefficient was computed by using Pearson correlation coefficient on the basis of 95% confidence level. It is found that there is very weak positive correlation coefficient of 0.08 with a P-value equal to 0.7. The P-value is greater than the significance level (α=0.05) of the 95% confidence level. This shows that the correlation is statistically non-significant. This very weak positive correlation shows that energetic particle precipitation (K-indices being used as a proxy) may not be responsible for PMSE echoes in this particular study. This result is opposite to that of Bremer et al. (2009) who found a non-significant, but strong positive correlation between PMSE-OR and geomagnetic indices.

Figure 5 shows the correlation between PMSE occurrence rate and Lyman α radiation. The analysis is restricted to only June and July. Here are only 10 data

points for each phenomenon because PMSE echoes were observed only in July for 2004, 2005, 2007, 2008, 2011, 2012, and 2015. PMSE echoes were only observed during June for year 2010, and both in June and July for year 2013. It is clear from the figure that the correlation is positive, but non-significant, since the Pearson linear correlation coefficient value of 0.42 is less than the critical value of Pearson correlation coefficient of 0.576 for a sample size n=10. The correlation of PMSE occurrence rate with Lyman α radiation is stronger than that with K-indices, which indicates that Lyman α radiation may be an important factor for PMSE echoes in this study. The possible explanation is that the Lyman α radiation can lead to enhance the ionization at altitudes 80–90 km and hence to enhance PMSE echoes. Our results supports the earlier finding by Bremer et al. (2009) and, Li and Rapp (2011) who used the data obtained with ALWIN radar at 53.5 MHz and 224 MHz, respectively and found positive correlation between PMSE occurrence and Lyman α radiation. This gives us important information that PMSE observed by radars of different frequencies show positive correlation with Lyman α radiation.
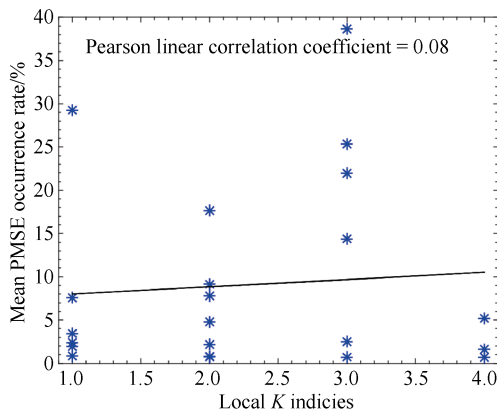

Figure 4   Correlation of PMSE occurrence rate with geomagnetic indices.
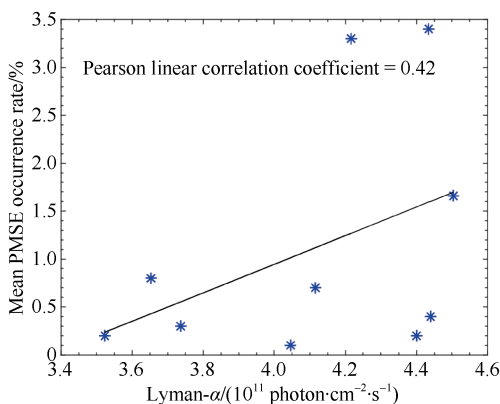

Figure 5   Correlation of PMSE occurrence rate with the solar Lyman-α radiation.

4.4   PMSE occurrence rate in different years and its correlation with NLC occurrence rate

The seasonal mean PMSE occurrence rates have been calculated using the data of June and July. Figure 6 shows the seasonal mean PMSE occurrence rate of different years observed by UHF radar. It is clear from this figure that for both the experiment modes, i.e., 'arcdlayer-ht' during the years 2004, 2005, 2007, 2008, and 'manda' during the years 2010–2013, 2015, there is a significant variations in the PMSE occurrence rate in different years. The possible reasons for variation in the PMSE occurrence rate in different years might be the variation in the NLC or Lyman alpha radiation responsible for ionization in the *D*-region.
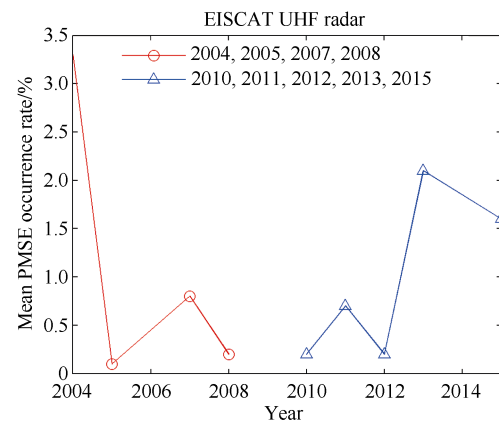

Figure 6   PMSE occurrence rate during the campaign of 'arcdlayer-ht' in 2004, 2005, 2007, 2008, and 'manda' in 2010–2013, 2015.

For comparing the PMSE occurrence rate with NLC occurrence rate, we have reproduced the NLC occurrence rate from observations with ALOMAR RMR lidar by Fiedler et al. (2017) and are over plotted in Figure 8. Figure 8 shows the comparison between PMSE and NLC occurrence rate. From this figure it is clear that there is matching between NLC and PMSE occurrence rates up to some extent. Moreover, we have computed the correlation between PMSE and NLC occurrence rate using the Pearson linear correlation coefficient. Figure 7 shows the correlation between PMSE and NLC occurrence rate. The NLC and PMSE occurrence rates are positively correlated having Pearson linear correlation coefficient of 0.41 with a *P*-value equal to 0.3. The *P*-value is greater than the significance level (α=0.05) of the 95% confidence level. This shows that the correlation is statistically non-significant. This positive correlation between the occurrence rate of NLC and PMSE echoes might support the expected reason proposed by Li and Rapp (2011) about the role of ice particle size in PMSE creation at high frequencies.

Moreover, there is a positive correlation between the Lyman α radiation and PMSE occurrence rate (see Figure 5), which shows that occurrence rate of PMSE at 930 MHz

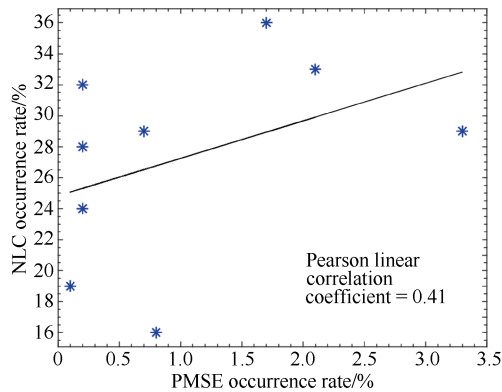increases with increasing ionization caused by Lyman α radiation.

Figure 7   Correlation between PMSE occurrence rates observed with EISCAT UHF radar and NLC occurrence rate with ALOMAR RMR lidar in different years i.e., 2004, 2005, 2007, 2008 and 2010–2013, 2015.
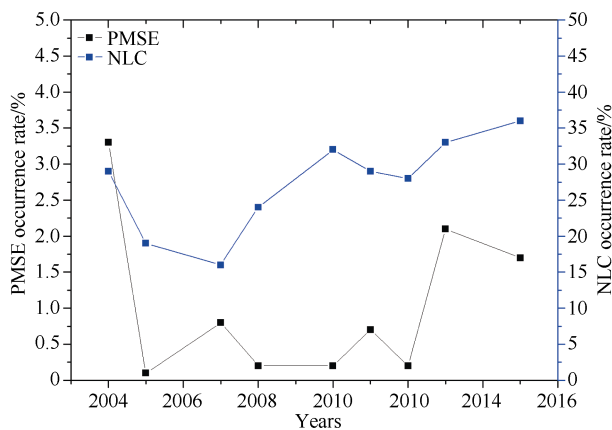

Figure 8   Comparison between PMSE occurrence rates observed with EISCAT UHF radar and NLC occurrence rate with ALOMAR RMR lidar in different years i.e., 2004, 2005, 2007, 2008 and 2010–2013, 2015.

5   Summary and conclusions

Based on the sporadic EISCAT UHF radar observations during the summer seasons from 2004 to 2015, we analyzed the temporal variation of PMSE occurrence, PMSE occurrence rate at different altitudes, correlation of PMSE occurrence with solar and geomagnetic activity, and finally the correlation of PMSE occurrence rate in different years with NLC occurrence rate. The main results can be summarized as follows:

(1) PMSE echoes were mostly observed in the early morning and fore-noon time, and have positive correlation with Lyman α radiation.

(2) Very weak positive but, statistically non-significant correlation is found between the local geomagnetic K-indices and PMSE occurrence rate.

(3) The occurrence rate of PMSE in different years is positively correlated with NLC occurrence rate.

References

Belova E, Dalin P, Kirkwood S. 2007. Polar mesosphere summer echoes: a comparison of simultaneous observations at three wavelengths. Ann Geophys, 25: 2487-2496, doi: 10.5194/angeo- 25-2487-2007.

Cho J Y N, Röttger J. 1997. An updated review of polar mesosphere summer echoes: Observation, theory and their relation to noctilucent clouds and subvisible aerosols. J Geophys Res, 102: 2001-2020, doi: 10.1029/96JD02030.

Croskey C L, Mitchell J D, Friedrich M, et al. 2001. Electrical structure of PMSE and NLC regions during the DROPPS program. Geophys Res Lett, 28: 1427-1430.

Ecklund W L, Balsley B B. 1981. Long-term observations of the Arctic mesopause with the MST radar at Poker Flat Alaska. J Geophys Res, 86: 7775-7780, doi: 10.1029/JA086iA09p07775.

Eremenko M N, Petelina S V, Zasetsky A V, et al. 2005. Shape and composition of PMC particles derived from satellite remote sensing measurements. Geophys Res Lett, 32(16): L16S06, doi: 10.1029/ 2005GL023013.

Fiedler J, Baumgarten G, Berger U, et al. Long-term variations of noctilucent clouds at ALOMAR. J Atmos Sol Terr Phys, 162: 79-89.

Folkestad K, Hagfors T, Westerlund S. 1983. EISCAT: An updated description of technical characteristics and operational capabilities. Radio Sci, 18: 867-879, doi: 10.1029/RS018i006p00867.

Gadsden M. 1981. The silver-blue clouds again: Nucleation and growth of ice in the mesosphere. Planet Space Sci, 29(10): 1079-1087, doi: 10.1016/0032-0633(81)90005-2.

Garcia R R, Solomon S. 1985. Effect of breaking gravity waves on the dynamics and chemical composition of the mesosphere and lower thermosphere. J Geophys Res, 90: 3850-3868, doi: 10.1029/JD090iD02 p03850.

Havnes O, Brattli A, Aslaksen T, et al. 2001. First common volume observations of layered plasma structures and polar mesospheric summer echoes by rocket and radar. Geophys Res Lett, 28(8): 1419-1422.

Hoppe U P, Hall C, Röttger J. 1988. First observations of summer polar mesospheric backscatter with a 224 MHz radar. Geophys Res Lett, 15: 28-31, doi: 10.1029/GL015i001p00028.

Kaifler N, Baumgarten G, Fiedler J, et al. 2011. Coincident measurements of PMSE and NLC above ALOMAR (69°N, 16°E) by radar and lidar from 1999–2008. Atmospheric Chem Phys, 11: 1355-1366, doi:

10.5194/acp-11-1355-2011.

Kelley M C, Farley D T, Röttger J. 1987. The effect of cluster ions on anomalous VHF backscatter from the summer polar mesosphere. Geophys Res Lett, 14: 1031-1034, doi: 10.1029/GL014i010p01031.

Latteck R, Bremer J. 2017. Long-term variations of polar mesospheric summer echoes observed at Andøya (69°N). J Atmos Sol Terr Phys, 163: 31-37.

Lehtinen M S, Huuskonen A. 1996. General incoherent scatter analysis and GUISDAP. J Atmos Terr Phys, 58: 435-452, doi: 10.1016/0021-9169 (95)00047-X.

Li Q, Rapp M. 2011. PMSE-observations with the EISCAT VHF and UHF-radars: Statistical properties. J Atmos Terr Phys, 73(9): 944-956, doi: 10.1016/j.jastp.2010.05.015.

Li Q, Rapp M. 2013. PMSE observations with the EISCAT VHF- and UHF-radars: Ice particles and their effect on ambient electron densities. J Atmos Sol Terr Phys, 104: 270-276, doi: 10.1016/j.jastp.2012.10.015.

Lübken F J, Berger U, Baumgarten G. 2013. Temperature trends in the midlatitude summer mesosphere. J Geophys Res, 118(24): 13347-13360, doi: 10.1002/2013JD020576.

Lübken F J, Lehmacher G, Blix T, et al. 1993. First in-situ observations of neutral and plasma density fluctuations within a PMSE layer. Geophys Res Lett, 20: 2311-2314, doi: 10.1029/93GL00851.

Lübken F J, Rapp M, Hoffmann P. 2002. Neutral air turbulence and temperatures in the vicinity of polar mesosphere summer echoes. J Geophys Res, 107 (D15): ACL 9-1-ACL 9-10, doi: 10.1029/ 2001JD000915.

Lübken F J, Zecha M, Höffner J, et al. 2004. Temperatures, polar mesosphere summer echoes, and noctilucent clouds over Spitsbergen (78° N). J Geophys Res, 109, D11203, doi: 10.1029/2003JD004247.

Mitchell J, Croskey C L, Goldberg R. 2001. Evidence for charged aerosol particles and associated meter-scale structure in identified PMSE/NLC regions. Geophys Res Lett, 28 (8): 1423-1426, doi: 10.1029/2000GL012685.

Næsheim L I, Havnes O, Lahoz C. 2008. A comparison of polar mesosphere summer echo at VHF (224 MHz) and UHF (930 MHz) and the effects of artificial electron heating. J Geophys Res, 113, D08205,

doi: 10.1029/2007JD009245.

Rapp M, Lübken F J. 2003. On the nature of PMSE: Electron diffusion in the vicinity of charged particles revisited. J Geophys Res, 108 (D8): 8437, doi: 10.1029/2002JD002857.

Rapp M, Strelnikova I, Latteck R, et al. 2008. Polar mesosphere summer echoes (PMSE) studied at Bragg wavelengths of 2.8 m, 67 cm, and 16 cm. J Atmos Sol Terr Phys, 70(7): 947-961, doi: 10.1016/j.jastp. 2007.11.005.

Röttger J, Lahoz C. 1990. Characteristics of polar mesosphere summer echoes (PMSE) observed with the EISCAT 224 MHz radar and possible explanations of their origin. J Atmos Sol Terr Phys, 52 (10-11): 893-906, doi: 10.1016/0021-9169(90)90023-G.

Röttger J, Rietveld M T, Lahoz C, et al. 1990. Polar mesosphere summer echoes observed with the EISCAT 933-MHz radar and the CUPRI 46.9 MHz radar, their similarity to 224 MHz radar echoes and their relation to turbulence and electron density profiles. Radio Sci, 25 (4): 671-687, doi: 10.1029/RS025i004p00671.

Thomas G E, Olivero J J, Jensen E J, et al. 1989. Relation between increasing methane and the presence of ice clouds in the mesopause. Nature, 338: 490-492, doi: 10.1038/338490a0

Thomas G E. 1991. Mesospheric clouds and the physics of the mesosphere region. Rev Geophys, 29: 553-575, doi: 10.1029/91 RG01604.

Thomas G E, Olivero J J. 2001. Noctilucent clouds as possible indicators of global change in the mesosphere. Adv Space Res, 28 (7): 937-946, doi: 10.1016/S0273-1177(01)80021-1.

Thomas G E, Olivero J J, Deland M, et al. 2011. Comment on "Are noctilucent clouds truly a "miner's canary" for global change? Eos Trans AGU, 84 (37): 352-353, doi: 10.1029/2003EO370008.

Varney R H, Nicolls M J, Heinselman C J, et al. 2009. Observations of polar mesospheric summer echoes using PFISR during the summer of 2007. J Atmos Sol Terr Phys, 71: 470-476.

Zahn U V. 2011. Are noctilucent clouds truly a ''miner's canary'' for global change? Eos Trans AGU, 84 (28): 261-264, doi: 10.1029/ 2003EO280001.